

June 25, 2010

Revised July 27, 2010

Higgs Mass Constraints on a Fourth Family: Upper and Lower Limits on CKM Mixing

Michael S. Chanowitz

*Theoretical Physics Group
Lawrence Berkeley National Laboratory
University of California
Berkeley, California 94720*

Abstract

Limits on the Higgs boson mass restrict CKM mixing of a possible fourth family beyond the constraints previously obtained from precision electroweak data alone. Existing experimental and theoretical bounds on m_H already significantly restrict the allowed parameter space. Zero CKM mixing is excluded and mixing of order θ_{Cabbibo} is allowed. Upper and lower limits on 3-4 CKM mixing are exhibited as a function of m_H . We use the default inputs of the Electroweak Working Group and also explore the sensitivity of both the three and four family fits to alternative inputs.

Introduction

A fourth family of quarks and leptons will be easy to discover or exclude at the LHC[1, 2] if the quark masses lie within the $m_Q \lesssim 500$ GeV domain defined by perturbative partial wave unitarity,[3] and even if they are too heavy to observe directly they will induce a large signal in $gg \rightarrow ZZ$ that will be clearly visible at the LHC.[4] A fourth family could be the key to many unsolved puzzles, such as the hierarchies of the fermion mass spectrum[5] including neutrino masses and mixing,[6] electroweak symmetry breaking,[7] baryogenesis,[8] and a variety of interesting phenomena in CP and flavor physics.[9] The four family Standard Model is likely to have a low cutoff above which new dynamics would emerge, which could be as low as $\sim 1\frac{1}{2}$ to 2 TeV if the quark masses are near the perturbative unitarity limit.[10, 11]

It has been known for a while that SM4, the four family Standard Model, is consistent with the precision electroweak (PEW) data,[12, 13, 14] as confirmed recently by two independent global fits.[15, 16] While SM4 does not greatly improve the quality of the fit (our best SM4 fit has χ^2 1.4 units lower than SM3), it can, as first noted in [13], resolve the tension with the LEP II 114 GeV lower limit on the Higgs boson mass that is especially acute if the A_{FB}^b anomaly is attributed to underestimated systematic error.[17] Primarily because of the A_{FB}^b anomaly, the Standard Model fit presented below, using EWWG inputs[18] (except Γ_W as noted below), has just a 14% confidence level, which can only be appreciably improved by new physics models with flavor nonuniversal interactions. As a result few of the new physics models under active consideration are able to raise the confidence level significantly.

In previous work we showed that CKM mixing of the fourth family is most effectively constrained by nondecoupling contributions to the ρ (or T) parameter, proportional to fourth family mixing angles and masses.[15] To constrain SM4 or any other BSM scenario, it is not sufficient to consider BSM perturbations around the SM best fit, but rather it is essential to perform global fits that vary both the SM and BSM parameters, since the best fit may occur at values of the SM parameters (especially m_H) that are quite different from their values in the SM best fit. In the previous work we followed the default procedures of the EWWG[18], including their data set, input parameters, and experimental correlations, implemented via the ZFITTER code[19] with two loop EW radiative corrections.[20] As expected our SM3 fit agrees very closely with the EWWG fit[21] (see below). For SM4 we found that fourth family CKM mixing of order θ_{Cabibbo} is allowed, leaving room for an SM4 explanation of possible flavor puzzles in the existing data. Our results have recently been confirmed by a second study using the same methodology.[22]

In this paper we incorporate recently obtained constraints on the SM4 Higgs boson mass into the PEW analysis. Because of the large enhancement of $gg \rightarrow H \rightarrow WW$ in SM4, CDF and D0 have been able to exclude the SM4 Higgs boson at 95% CL for $131 \leq m_H \leq 204$ GeV.[23] As shown below this constraint combined with the EW fit and the LEP II

limit on m_H excludes a large portion of the SM4 parameter space with small or vanishing fourth family CKM mixing. A potentially stronger, theoretical constraint follows from the RG/stability analysis of Hashimoto who showed for zero CKM4 mixing that $m_H \gtrsim m_{Q_4}$ must be approximately satisfied to assure the existence of a region between the fourth family quark mass scale and the scale of new physics in which SM4 is a valid effective theory amenable to perturbation theory.[11] Combined with the PEW data this result excludes vanishing and very small CKM4 mixing. The generalization of Hashimoto’s inequality to nonvanishing CKM4 mixing could provide significant upper and lower bounds on fourth family mixing angles, depending on the sign and magnitude of the CKM angle dependent corrections. The lower bound on CKM4 mixing has a simple explanation: larger values of m_H cause the fit to favor larger mixing, because increased mixing induces an increase in the oblique parameter T that offsets the decrease due to larger m_H .

The PEW fits depend of course on the inputs, including the choice of data set and especially $\Delta\alpha^{(5)}$, the five flavor hadronic contribution to the running of α to the Z pole, which is the dominant uncertainty in $\alpha(m_Z)$. While it is reasonable to consider alternate inputs, the EWWG inputs continue to be a valid, conservative choice in view of existing systematic uncertainties. A study using different inputs[16] evidently favored tighter constraints on CKM4 mixing, although no explicit limits on mixing angles were presented. To illustrate the sensitivity of the results to the inputs we explore alternatives to the EWWG defaults: we consider two recent determinations of $\Delta\alpha^{(5)}$, an augmented data set with low energy measurements, and a reduced set which omits the hadronic asymmetry measurements. In all cases we find that zero CKM4 mixing is excluded and that CKM4 mixing of order θ_{Cabbibo} is allowed at 95% CL, although when one of the $\Delta\alpha^{(5)}$ choices is applied to the data without hadronic asymmetries only small regions of the parameter space are allowed.

In the next section we briefly review the SM3 fit and illustrate the effect of alternative inputs. We then present the EW and Higgs mass constraints on CKM4 mixing, including the two loop[24] nondecoupling contributions $\propto m_{Q_4}^2$ to both T and the $Z\bar{b}b$ vertex. For simplicity we assume 3-4 mixing is dominant; the straightforward generalization to also include 2-4 or 1-4 mixing was given in our previous work.[15] We conclude with a brief discussion of some of the many aspects of the SM4 scenario that remain to be explored.

SM Fits

In this section we compare our SM3 fit to the most recent SM fit of the EWWG and then compare the impact of various alternative inputs. In particular we consider two alternates for $\Delta\alpha^{(5)}$ and vary the data set by adding low energy measurements to the “high energy” set of the EWWG or by removing the hadronic asymmetry measurements as suggested by one possible interpretation of the A_{FB}^b anomaly reviewed below.

	Experiment	EWVG	Pull	I	Pull
$\Delta\alpha^{(5)}(m_Z)$	0.02758 (35)	0.02768	-0.3	0.2768	-0.3
m_t	173.1 (1.3)	173.2	-0.1	173.3	-0.1
$\alpha_S(m_Z)$		0.1185		0.1180	
m_H		87		89	
χ^2/dof		17.3/12		17.3/12	
$\text{CL}(\chi^2)$		0.14		0.14	
$m_H(95\%)$		155		150	
$\text{CL}(m_H > 114 \text{ GeV})$				0.23	
A_{LR}	0.1513 (21)	0.1481	1.5	0.14804	1.55
A_{FB}^l	0.01714 (95)	0.0165	0.7	0.1644	0.7
$A_{e,\tau}$	0.1465 (33)	0.1481	-0.5	0.14804	-0.5
A_{FB}^b	0.0992 (16)	0.1038	-2.9	0.1038	-2.9
A_{FB}^c	0.0707 (35)	0.0742	-1.0	0.0742	-1.0
Q_{FB}	0.23240 (120)	0.23138	0.8	0.23139	0.8
Γ_Z	2495.2 (23)	2495.9	-0.3	2495.7	-0.2
R_ℓ	20.767 (25)	20.742	1.0	20.739	1.1
σ_h	41.540 (37)	41.478	1.7	41.481	1.6
R_b	0.21629 (66)	0.21579	0.8	0.21582	0.7
R_c	0.1721 (30)	0.1723	-0.1	0.1722	-0.04
A_b	0.923 (20)	0.935	-0.6	0.935	-0.6
A_c	0.670 (27)	0.668	0.1	0.668	0.07
m_W	80.399 (23)	80.379	0.9	80.378	0.9

Table 1: Comparison of our SM fit with EWWG defaults to the summer 2009 EWWG fit.[21] The 95% upper limit on m_H for the EWWG fit reflects the “blue band” systematic uncertainties while our value does not.

Table 1 compares our SM fit with EWWG inputs,¹ labeled fit **I**, to the experimental data and to the EWWG summer 2009 fit.[21] The first four rows display the parameters which are scanned in the fits and are the inputs to the calculation of the radiative corrections of the other observables.² We follow the EWWG practice of allowing the strong coupling constant α_S to float unconstrained; the fits are not very sensitive to its precise value as long as it is within $\sim 2\%$ of 0.118, as for instance in the PDG fit of α_S . [25] The χ^2 values and confidence levels are shown in the next two rows. The two fits are virtually identical.

The acceptable but somewhat marginal 14% CL in table 1 is due to the 3.2σ discrepancy between the two most precise determinations of $\sin^2\theta_W^{\text{eff}}$ from A_{FB}^b and A_{LR} , which are seen to have pulls of opposite sign. The largest pull, 2.9σ , is borne by A_{FB}^b because of an “alliance” of A_{LR} and the other leptonic asymmetry measurements with m_W , which prefer values of m_H near 50 GeV, while A_{FB}^b and the other hadronic asymmetry measurements favor $m_H \simeq 500$ GeV. A possible explanation that cannot be excluded *a priori* is that the hadronic asymmetries have underestimated systematic uncertainties,[17] for which a leading candidate is the merging, estimated by hadronic Monte Carlo, of the large QCD radiative corrections with the experimental acceptance[26] (see the talk cited at [17]) for a recent discussion). The anomaly could then be a signal of new physics to raise the predicted value of the Higgs mass above the 50 GeV scale predicted in the SM by the leptonic asymmetries and m_W .

To explore the effect of alternative inputs we begin by considering the EWWG data set of table 1 but with two different, recently obtained values for $\Delta\alpha^{(5)}$. The results are summarized in table 2, where we display the input values for $\Delta\alpha^{(5)}$ and the corresponding best fit results for the four scanned parameters ($\Delta\alpha^{(5)}$, m_t , α_S , and m_H) that control the radiative corrections. Fit **I** is the same fit shown in table 1 with the EWWG default $\Delta\alpha^{(5)}$. [27] The fit **II** value of $\Delta\alpha^{(5)}$ [28] uses a BABAR analysis of radiative return data to determine $\sigma(e^+e^- \rightarrow \text{hadrons})$ in the poorly known region between 1.4 and 2 GeV. The result is almost identical to the EWWG default but with a much smaller quoted error. The fit **III** value of $\Delta\alpha^{(5)}$, [29] which was used in the SM4 fits reported in [16], uses tau decay data as well as the BABAR data. The resulting $\Delta\alpha^{(5)}$ has a larger central value and a much smaller quoted error than the EWWG default.³ The values of $\Delta\alpha^{(5)}$ in **II** and **III** differ by almost 2σ . Fits **I** and **II** in table 2 are nearly identical, indicating that the increased precision of the fit **II**

¹We omit Γ_W ; with 2.5% uncertainty it does not approach the part per mil accuracy typical of the other precision data and has little effect on the fit.

² G_F and m_Z are also inputs to the radiative corrections. Because they are known much more precisely than the other quantities the fits do not change if they are scanned and so they are just set to their central values.

³In [29] the three-flavor contribution $\Delta\alpha^{(3)}$ is computed and then RG extrapolated to the Z -pole. To a good approximation the result corresponds to the value of $\Delta\alpha^{(5)}$ given in table 2.[30]

	I	II	III
$\Delta\alpha^{(5)}(m_Z)$ input	0.02758 (35)	0.02760 (15)	0.02793(11)
$\Delta\alpha^{(5)}(m_Z)$	0.02768	0.02761	0.02797
m_t	173.3	173.3	173.3
$\alpha_S(m_Z)$	0.118	0.118	0.1186
m_H	89	94	74
χ^2/dof	17.3/12	17.3/12	16.8/12
$\text{CL}(\chi^2)$	0.14	0.14	0.16
$m_H(95\%)$	150	146	123
$\text{CL}(m_H \geq 114 \text{ GeV})$	0.23	0.22	0.08

Table 2: Comparison of SM3 fits to the EWWG data set for three input values of $\Delta\alpha^{(5)}(m_Z)$.

$\Delta\alpha^{(5)}$ does not have a major impact on the best fit. The higher central value of $\Delta\alpha^{(5)}$ in fit **III** does have an appreciable effect, pulling m_H to smaller values, with the 95% CL upper limit at 123 GeV, and creating tension with the LEP II 114 GeV lower limit, with which it is inconsistent at 92% CL. Figure 1 shows χ^2 plotted as a function of m_H for the three fits, with 90% symmetric confidence intervals indicated by the horizontal lines.

Next we consider the effect of adding low energy data to the EWWG data set. There are three candidates that might appreciably affect the fit of m_H : the weak charge Q_W of the ^{133}Cs nucleus measured in atomic parity violation and the measurements of $\sin^2\theta_W$ in Möller scattering at SLAC[31] and in νN scattering by the NuTeV collaboration.[32] In the past the EWWG has included the APV and NuTeV measurements but eventually omitted them from the fit because of concerns about systematics. Today the original NuTeV result is no longer relevant because of a subsequent measurement by the NuTeV collaboration of an asymmetry in the nucleon $\bar{s}s$ sea[33] as well as changes in several other related measurements. For the fits in [16] the NuTeV result was revised with four modifications of the original analysis; we prefer to omit the NuTeV measurement pending an authoritative analysis by the NuTeV collaboration itself. In any case the omission has little effect on the results.

A recent calculation[34] of Cesium atomic transitions claims a significantly reduced theoretical uncertainty and the central value, which has previously disagreed with the SM by 2σ , now agrees almost precisely (with $Q_W = -73.16 \pm 0.29 \pm 0.20$ while our SM fit yields $Q_W = -73.14$) and therefore contributes zero to the χ^2 . The error estimate is tested by comparing calculations of several supporting quantities with experiment.[35] We include this new APV result and also the Möller scattering measurement, which translated to the Z -pole is $\sin^2\theta_W^{\ell\text{eff}} = 0.23339 \pm 0.00140$. [25] It provides a less precise value of $\sin^2\theta_W^{\ell\text{eff}}$ than Q_{FB} ,

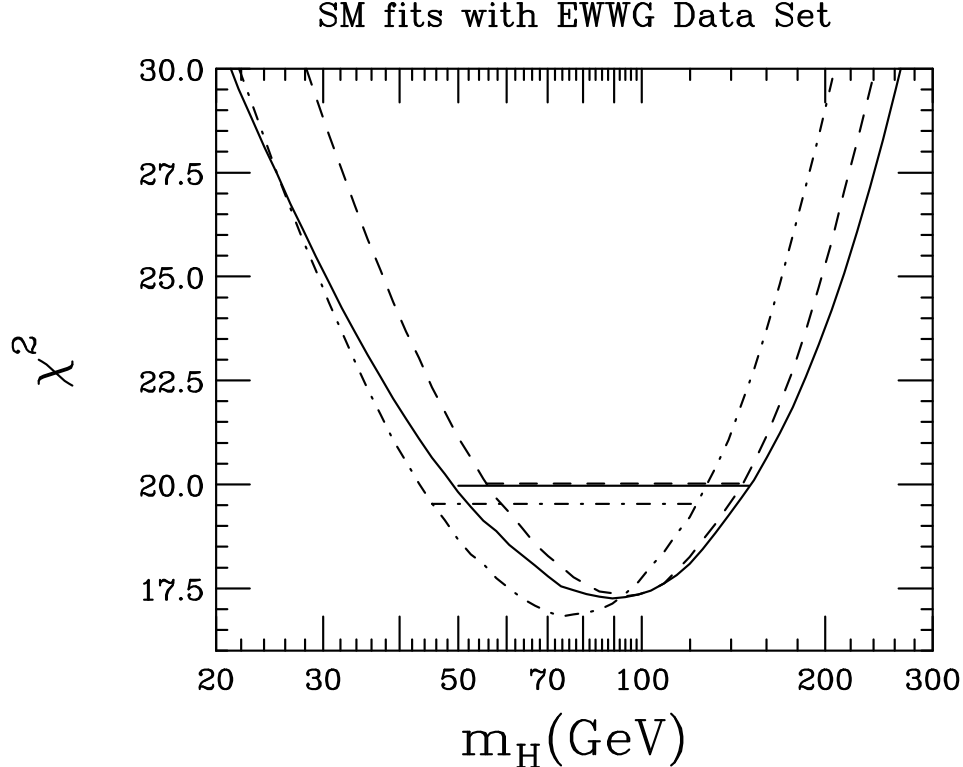


Figure 1: $\chi^2(m_H)$ for the SM fits in table 2: **I** solid, **II** dashed, and **III** dash-dot. The horizontal lines indicate the symmetric 90% confidence intervals.

which is the least precise of the six Z decay asymmetry measurements in table 1. In the SM fits the Möller measurement has a pull of 1.4σ and tends to slightly increase m_H .

Fits including the low energy measurements are shown in table 3. The low energy data has little effect except for the very small increase in m_H . The χ^2 increases by two for the two additional degrees of freedom and the χ^2 confidence levels hardly change. Fit **III** continues to exhibit tension with the LEP II lower limit on m_H . If we include the NuTeV measurement as revised in [16] the only effect on the fits is another very slight increase in m_H , e.g., for fit **III** the 95% CL upper limit increases from 127 to 130 GeV and the CL for $m_H > 114$ GeV increases from 0.10 to 0.11.

Table 4 shows the effect of removing the three hadronic asymmetry measurements from the EWWG data set, as would be appropriate if the A_{FB}^b anomaly results from underestimated systematic error.[17] The χ^2 CL's increase to robust levels but the m_H predictions fall significantly below the LEP II lower limit. The conflict is most acute for fit **III**, which is inconsistent with the LEP II limit at 99.65% CL. Conflict between the fit and the direct limit could be a signal of new physics to increase the m_H prediction, as occurs generically for new physics models with $T > 0$, for example, in SM4.

	I	II	III
$\Delta\alpha^{(5)}(m_Z)$ input	0.02758 (35)	0.02760 (15)	0.02793(11)
$\Delta\alpha^{(5)}(m_Z)$	0.02768	0.02761	0.02797
m_t	173.3	173.3	173.3
$\alpha_S(m_Z)$	0.118	0.118	0.1186
m_H	94	99	74
χ^2/dof	19.3/14	19.3/14	18.8/14
$\text{CL}(\chi^2)$	0.16	0.16	0.17
$m_H(95\%)$	154	150	127
$\text{CL}(m_H \geq 114 \text{ GeV})$	0.25	0.25	0.10

Table 3: Comparison of SM3 fits to the EWWG data set plus low energy measurements ($Q_W(Cs)$ and Möller scattering) for three input values of $\Delta\alpha^{(5)}(m_Z)$.

To summarize this section, the greatest changes to the SM fit from the alternatives to the EWWG defaults that we have considered arise from the $\Delta\alpha^{(5)}$ of fit **III** and from the exclusion of the hadronic asymmetry measurements, while the increased precision of the fit **II** $\Delta\alpha^{(5)}$ and the addition of the low energy measurements have less impact.

SM4 Fits and Higgs mass constraints

We now consider the correlated constraints on CKM4 mixing that result from the combination of recent SM4 Higgs mass constraints with the constraints from the precision EW data. We assume for simplicity that the fourth family mixes predominantly with the third and will exhibit the 95% CL allowed regions in the $s_{34} - m_H$ plane, where $s_{34} = \sin\theta_{34}$ is the sine of both the $t' - b$ and $b' - t$ mixing angles. Following [16] we choose $m_{t'} - m_{b'} = 16$ GeV and $m_{\tau'} - m_{\nu'} = 91$ GeV, yielding a slightly lower χ^2 (by ~ 0.5) than the masses used in [15] which were based on the fits of [14]. We fix $m_{\nu'} = 101$ GeV and consider two choices for the quark masses, $m_{b'} = 338$ GeV, which is at the current CDF[36] lower limit,⁴ and $m_{b'} = 484$ GeV corresponding to $m_{t'} = 500$ GeV, at the perturbative unitarity limit.[3] In addition to the leading one loop nondecoupling contributions to T and the $Z\bar{b}b$ vertex proportional to $m_{Q_4}^2$ we also include the leading nondecoupling two loop contributions proportional to $m_{Q_4}^4$. [24] As shown in [15], perturbation theory for the nondecoupling corrections remains under control for $m_{t'} = 500$ GeV but has decisively broken down at $m_{t'} = 1$ TeV. In addition to the EWWG defaults we consider alternative inputs as in the previous section.

⁴The CDF limit on $m_{b'}$ assumes $b' \rightarrow tW$ is dominant and prompt. For other scenarios other limits will apply — see [37].

	I	II	III
$\Delta\alpha^{(5)}(m_Z)$ input	0.02758 (35)	0.02760 (15)	0.02793(11)
$\Delta\alpha^{(5)}(m_Z)$	0.02761	0.02761	0.02790
m_t	173.3	173.3	173.3
$\alpha_S(m_Z)$	0.118	0.118	0.118
m_H	52	52	45
χ^2/dof	5.59/9	5.59/9	5.76/9
$\text{CL}(\chi^2)$	0.78	0.78	0.76
$m_H(95\%)$	105	94	80
$\text{CL}(m_H \geq 114 \text{ GeV})$	0.030	0.016	0.0035

Table 4: Comparison of SM3 fits to the EWWG data set minus the three front-back hadronic asymmetry measurements for three input values of $\Delta\alpha^{(5)}(m_Z)$.

The 95% CL $s_{34} - m_H$ contours ($\Delta\chi^2 = 5.992$) are defined with respect to the best fit for each set of fourth family masses and fit inputs, which always occurs at $s_{34} = 0$. The best fits for the parameter set with $m_{t'}, m_{b'} = 354, 338$ GeV are shown in table 5 for the EWWG data set with the three values of $\Delta\alpha^{(5)}$ considered above. The χ^2 confidence level is defined in a Bayesian sense, assuming that the fourth family masses are known *a priori*. Comparing with the corresponding SM3 fits in table 2, we see that the χ^2 is slightly lower, by $\Delta\chi^2 = -0.6$, for SM4 fits **I** and **II** than for the corresponding SM3 fits and slightly higher (+0.2) for fit **III**. The difference probably reflects the strong preference of the fit **III** $\Delta\alpha^{(5)}$ for small m_H seen in the SM3 fits of the previous section, since positive T in the SM4 fits puts “upward pressure” on m_H . This effect is more pronounced in the 95% contour plots shown below. The best fits including the low energy measurements are very similar and are not displayed. The fits with $m_{t'}, m_{b'} = 500, 484$ GeV and $s_{34} = 0$ are also virtually identical to those of table 5 and are also not displayed.

The sensitivity of the fits to θ_{34} arises from nondecoupling heavy fermion contributions to the $Z\bar{b}b$ vertex correction[38, 39] and, predominantly, to the oblique parameter T , given at one loop by[15]

$$T_4 = \frac{1}{8\pi x_W(1-x_W)} \left\{ 3 [F_{t'b'} + s_{34}^2(F_{t'b} + F_{b't'} - F_{tb} - F_{t'b'})] + F_{l_4\nu_4} \right\}. \quad (1)$$

and

$$\delta^V g_{bL}^{3-4} = s_{34}^2 \frac{\alpha}{16\pi x_W(1-x_W)} \left(\frac{m_{t'}^2}{m_Z^2} - \frac{m_t^2}{m_Z^2} \right) \quad (2)$$

	I	II	III
$\Delta\alpha^{(5)}(m_Z)$ input	0.02758 (35)	0.02760 (15)	0.02793(11)
$\Delta\alpha^{(5)}(m_Z)$	0.02754	0.02761	0.02790
m_t	173.3	173.3	173.3
$\alpha_S(m_Z)$	0.1174	0.1174	0.1174
m_H	114	109	89
χ^2/dof	16.7/12	16.7/12	17.0/12
$\text{CL}(\chi^2)$	0.16	0.16	0.15

Table 5: SM4 fits to the EWWG data set with $m_{t'}, m_{b'} = 354, 338$ GeV, $S, T = 0.139, 0.159$ and $s_{34} = 0$, for three values of $\Delta\alpha^{(5)}$.

where $x_i = m_i^2/m_Z^2$, $x_W = \sin^2\theta_W^2$, and

$$F_{12} = \frac{x_1 + x_2}{2} - \frac{x_1 x_2}{x_1 - x_2} \ln \frac{x_1}{x_2} \quad (3)$$

is the well known nondecoupling fermionic correction to the rho parameter.[40, 3]

Figures 2 and 3 display the 95% CL contours for $m_{t'} = 354$ and $m_{t'} = 500$ GeV respectively, for the EWWG data set both with and without the addition of the low energy measurements, and for the three values of $\Delta\alpha^{(5)}$ considered previously. The contour bounded by the solid line corresponds to the EWWG default data set and default value for $\Delta\alpha^{(5)}$, labeled as fit **I** in table 5. The dotted line that lies just within the solid contour is the result of adding the low energy measurements to the data set, seen to have an almost negligible effect. Similarly the dashed and dot-dashed contours and their accompanying dotted lines are the result of the fit **II** and fit **III** $\Delta\alpha^{(5)}$ values respectively. As m_H increases above 250 GeV the fits imply both lower and upper limits on $|s_{34}|$. For instance, at $m_H = m_{t'} = 354$ GeV, the fit **I** contour restricts θ_{34} to the interval $0.115 \leq |s_{34}| \leq 0.225$. Similarly for fit **I** at $m_H = m_{t'} = 500$ GeV, θ_{34} is restricted to $0.07 \leq |s_{34}| \leq 0.14$. As was the case for the SM3 fits, we see that the fit **I** and fit **II** contours are very similar, with nearly identical upper limits on $|s_{34}|$ although fit **II** yields a more restrictive lower limit. In both cases the reach in m_H extends to 1 TeV and the upper limit on s_{34} extends to $\simeq 0.26$ for $m_{t'} = 354$ GeV and to $\simeq 0.17$ for $m_{t'} = 500$ GeV.

As was the case for the SM3 fits the most significant effect of the alternative inputs is from the fit **III** value of $\Delta\alpha^{(5)}$. The fit **III** contours for the upper limit of $|s_{34}|$ follow those of fits **I** and **II** quite closely until $m_H = 690$ (660) GeV, for figure 1 (2), which shows that the somewhat tighter upper limit on $|s_{34}|$ in fit **III** is a consequence of the well known correlation between larger $\Delta\alpha^{(5)}$ and smaller values of m_H that we saw in the SM3 fits of

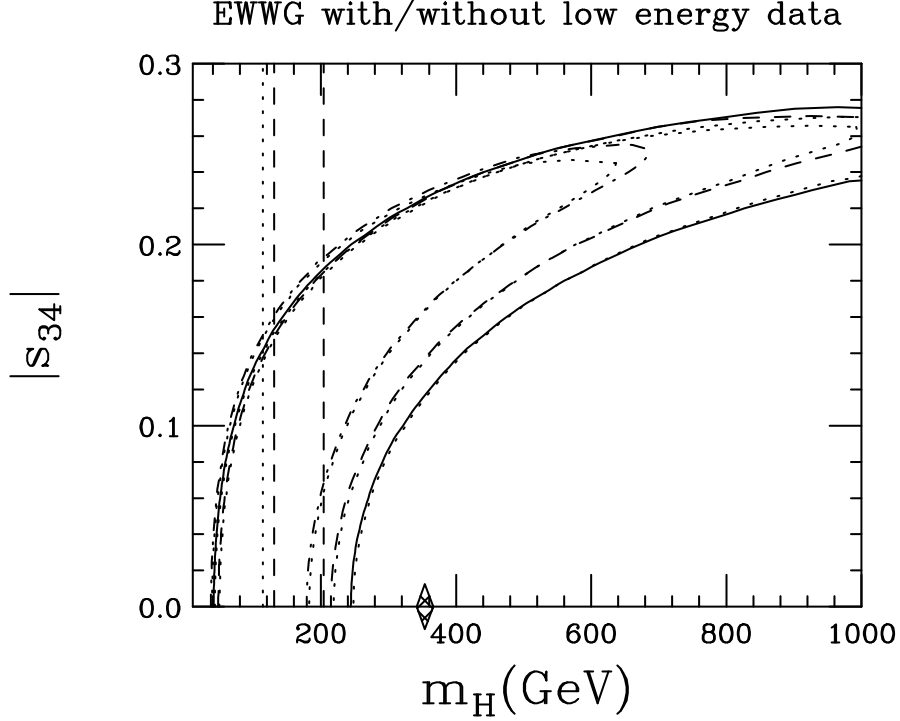


Figure 2: 95% CL contour plots for SM4 with $m_{t'}, m_{b'} = 354, 338$ GeV: **I** solid, **II** dashed, and **III** dash-dot. The nearly identical dotted contours include the low energy data. The vertical dotted and dashed lines indicate the LEP II and Tevatron 95% exclusion regions, and the diamond on the abscissa marks the stability bound $m_H \gtrsim m_{t'}$.

the previous section. For $m_H \lesssim 600$ GeV the upper limit on $|s_{34}|$ is nearly the same for all three fits although the lower limits from fits **II** and **III** are stronger. In particular, for $m_H = m_{t'} = 354$ GeV and $m_H = m_{t'} = 500$ GeV, the upper limit on $|s_{34}|$ is nearly the same for all three $\Delta\alpha^{(5)}$ inputs, with or without the low energy data.

The direct experimental limits on m_H are indicated by the vertical lines in figures 2 and 3, and a theoretical limit is indicated by the diamond on the abscissa at $m_H = m_{t'}$. The dotted vertical line denotes the LEP II 95% CL lower limit and the region between the two dashed vertical lines marks the 131 – 204 GeV SM4 95% CL exclusion region established by CDF and D0. Except for the interval between 114 and 131 GeV we see that $\theta_{34} = 0$ is excluded by fit **III** and is nearly excluded by fit **II**, and that fit **III** requires $0.255 > |s_{34}| > 0.065$ for $m_{t'} = 354$ GeV and $0.16 > |s_{34}| > 0.035$ for $m_{t'} = 500$ GeV. The lower limits on $|s_{34}|$ will be strengthened as the limits on the SM4 Higgs boson are tightened at the Tevatron and the LHC (or when it is discovered!).

The theoretical lower limit on m_H indicated by the diamond in figures 2 and 3 at $m_H = m_{t'}$ applies strictly speaking only at $\theta_{34} = 0$, but it is safe to say that it also excludes at least

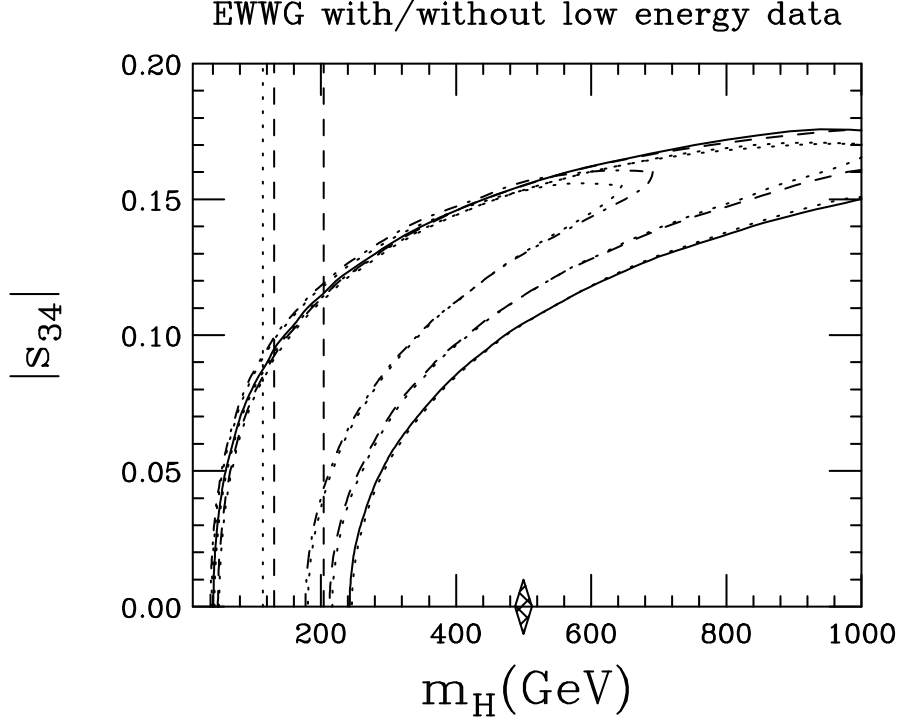


Figure 3: 95% CL contour plots for SM4 with $m_{t'}, m_{b'} = 500, 484$ GeV, as in figure 2.

some small region around $\theta_{34} = 0$. The bound $m_H \gtrsim m_{t'}$ follows from the assumption that the cutoff for new BSM4 physics is no lower than 2 TeV, and can be relaxed to $m_H \gtrsim m_{t'} - 50$ GeV if the cutoff is lowered to 1 TeV.[11] Since the analysis of [11] was performed assuming $\theta_{34} = 0$, we cannot be sure how it affects the allowed region of the entire $|s_{34}| - m_H$ plane. Assuming that the bound for $\theta_{34} \neq 0$ is of the form $m_H \gtrsim m_{t'}(1 + C|s_{34}|)$, the sign and value of the coefficient C will determine the further restrictions on $|s_{34}|$; if it is of the form $m_H \gtrsim m_{t'}(1 + C|s_{34}|^2)$ the corrections will be small. If the s_{34} correction is quadratic or if C is very small the entire region $m_H \lesssim m_{t'}$ would be excluded and the allowed region would establish lower and upper limits on $|s_{34}|$, which for the EWWG defaults, fit **I**, would be $0.275 > |s_{34}| > 0.115$ for $m_{t'} = 354$ GeV and $0.175 > |s_{34}| > 0.105$ for $m_{t'} = 500$ GeV.

Figures 4 and 5 show the contour plots for the data set consisting of the EWWG “high energy” measurements listed in table 1 but without the three hadronic asymmetry measurements, A_{FB}^b , A_{FB}^c , and Q_{FB} , as would be appropriate if the A_{FB}^b anomaly is due to underestimated systematic error. The corresponding SM3 fits were summarized in table 4. We see from figures 4 and 5 that SM4 removes the tension with the 114 GeV LEP II lower limit on m_H that is apparent in table 4, but that in the case of fit **III** the CDF-D0 limit on the SM4 Higgs boson mass excludes most of the remaining allowed parameter space except for two small regions between 114 and 131 GeV and between 204 and 230 GeV. Fits **I** and **II** have extensive allowed regions above $m_H = 204$ GeV but depending on how mixing

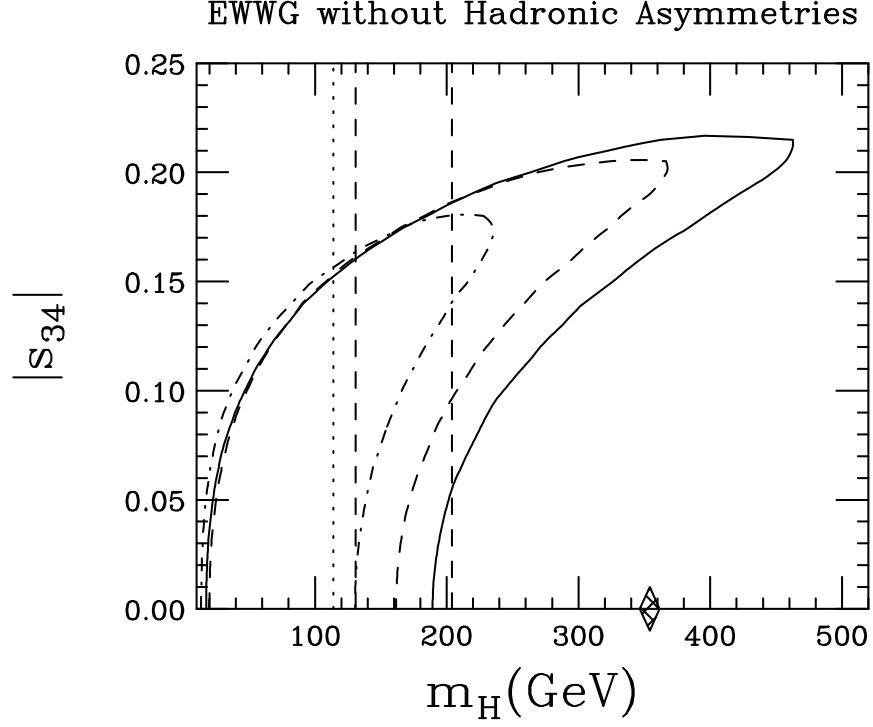


Figure 4: SM4 95% CL contour plots with $m_{t'}, m_{b'} = 354, 338$ GeV, as in figure 2, without the three hadronic asymmetry measurements.

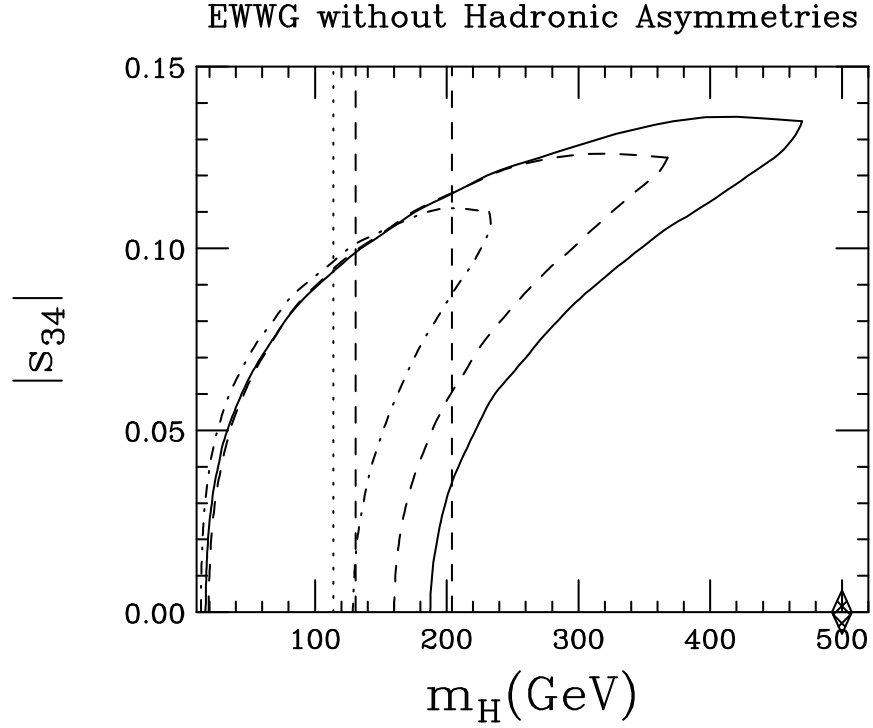


Figure 5: SM4 95% CL contour plots with $m_{t'}, m_{b'} = 500, 484$ GeV, as in figure 2, without the three hadronic asymmetry measurements.

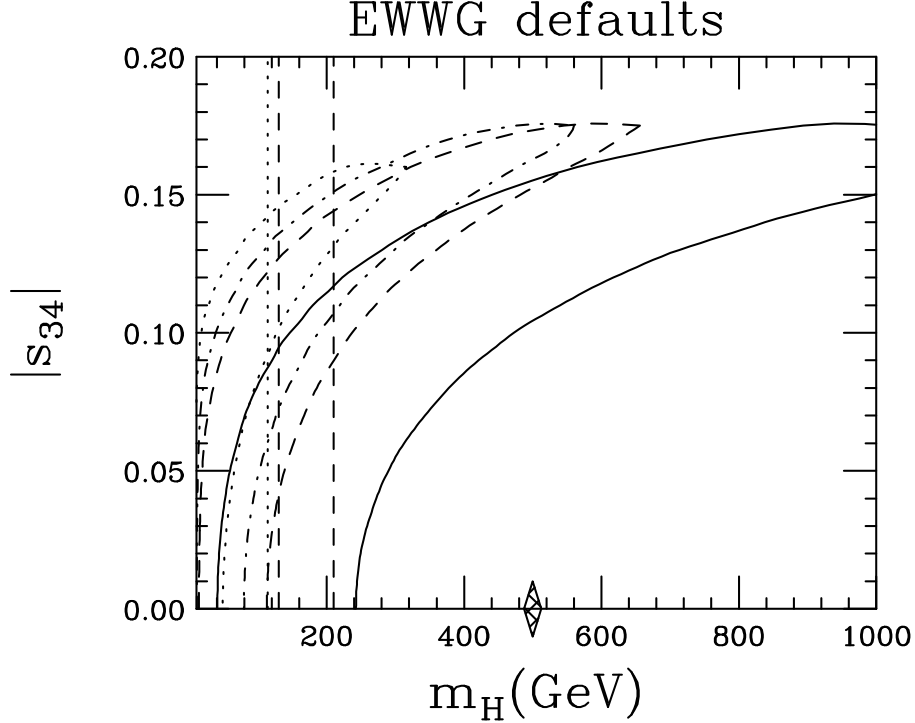


Figure 6: 95% CL contours as in figure 2 using EWWG defaults, all with $m_{t'} = 500$ GeV and $m_{\nu'} = 100$ GeV. For the dotted and dash-dotted contours $m_{b'} = 500$ GeV while $m_{\ell'} - m_{\nu'} = 0$ and 40 GeV respectively. The dashed contour is for the best fit model described in the text, with $m_{b'} = 475$ GeV and $m_{\ell'} - m_{\nu'} = 45$ GeV. The solid contour, reproduced from figure 3, is for $m_{b'} = 484$ GeV and $m_{\ell'} - m_{\nu'} = 91$ GeV.

affects the theoretical lower limit on m_H , i.e., the parameter C discussed above, they could be severely constrained or even entirely excluded by the theoretical limit.

The quark and lepton masses considered above were chosen because they yield good fits for $s_{34} = 0$. We may then ask whether different masses might provide better fits for $s_{34} \neq 0$. Since the decrease in confidence level for increasing $|s_{34}|$ is a consequence of the associated increase in T , it might seem that quark and lepton doublets with smaller mass splittings could yield improved fits at large $|s_{34}|$ even if they are not favored at $s_{34} = 0$. We find however that this strategy does not increase the upper limit on $|s_{34}|$ although it does change the relationship between s_{34} and m_H . The quark mass splitting used above, $m_{t'} - m_{b'} = 16$ GeV, results in a very small value of $F_{t'b'}$, two orders of magnitude smaller than F_{tb} and three orders of magnitude smaller than $F_{t'b}$ for $m_{t'} = 500$ GeV, so that the resulting fits are nearly identical to those with $m_{t'} = m_{b'}$. Thus the only possibility to pursue this strategy is to reduce the lepton mass splitting from the 91 GeV value used in the fits presented above.

We illustrate this strategy with two models, taking $m_{t'} = m_{b'} = 500$ GeV, $m_{\nu'} = 100$

GeV and $m_{\ell'} - m_{\nu'} = 0$ or 40 GeV. Unlike the cases considered above, in these models χ^2 does not increase monotonically from a minimum at $s_{34} = 0$. Instead the χ^2 minimum occurs at $|s_{34}| \simeq 0.06$ but at unacceptably small Higgs masses, around 30 to 40 GeV. The 95% CL contours are shown in figure 6 (dots and dash-dots) where they are compared to the model with $m_{\ell'} - m_{\nu'} = 91$ GeV (solid). We see that the upper limit on $|s_{34}|$ is not increased and that the allowed parameter space is significantly reduced by the Higgs mass constraints. The preference for small m_H in these fits is a consequence of the interplay between the oblique parameters S and T with the Higgs mass: decreasing the mass splittings reduces T and increases S , which both drive the fit to small m_H . Though the parameter space is reduced these models are currently still viable. They do not achieve larger upper limits on $|s_{34}|$, but they do allow larger mixing at smaller m_H .

Finally we consider the masses that yield the lowest χ^2 minimum we have obtained using EWWG defaults. Fixing $m_{t'} = 500$ GeV and $m_{\nu'} = 100$ GeV, we find that the smallest χ^2 occurs for $m_{t'} - m_{b'} \simeq 25$ GeV, $m_{\ell'} - m_{\nu'} \simeq 40$ GeV, and $s_{34} = 0$. The value at the minimum, $\chi^2 = 15.9$, is 1.4 units less than the SM3 best fit, for which the minimum is $\chi^2 = 17.3$ (see table 1). While this model has the deepest χ^2 minimum we have found and that minimum occurs at $s_{34} = 0$, the upper limit $|s_{34}| \lesssim 0.175$ is as large as that of any of the other models, as seen in the dashed contour in figure 6. The allowed range of CKM4 mixing is not extended by tuning masses to move the χ^2 minimum to $s_{34} \neq 0$.

Discussion

We have explored the constraints on fourth family CKM mixing that arise from the combined effect of the precision electroweak data and bounds on the mass of the SM4 Higgs boson. We find that fourth family CKM mixing of order θ_{Cabbibo} is allowed, with $|s_{34}| \lesssim 0.27$ for quark masses near the Tevatron lower limit and with $|s_{34}| \lesssim 0.17$ for masses near the perturbative unitarity upper limit, and that the experimental and theoretical bounds on m_H in SM4 favor nonvanishing fourth family CKM mixing. In addition to the EWWG default inputs we explored alternate data sets and values of $\Delta\alpha^{(5)}$. Adding low energy data has little effect but removing the hadronic front-back asymmetries leads to much tighter constraints. One recent determination[28] of $\Delta\alpha^{(5)}$ yields very similar results to the EWWG default fits while another[29, 16] strongly prefers small m_H , causing tension with the LEP II 114 GeV lower limit in SM3 and a tighter upper limit on m_H in SM4. A possible explanation of the difference is that [29] uses τ decay data, while [28] does not because of concern over systematic uncertainties associated with the isospin corrections required in the τ analysis. It would be interesting to know the extent to which the τ data influences the result in [29].

This work is restricted to the implications of the precision EW data and the Higgs mass limits on CKM mixing in SM4. In a truly global approach data from two other areas should also be confronted. Lacker and Menzel have made the interesting observation that

the extraction of G_F in SM4 leaves room for significant deviations from its value in SM3 which would affect the analysis of the precision EW data, and that the CKM4 and PMNS4 matrices should be considered simultaneously in a single fit.[41] The EW fit of the CKM4 matrix can also be extended by including FCNC and CP constraints together with the EW constraints, and a first step in this direction has been taken.[42] Both are clearly important directions to pursue.

The effect of the Higgs boson mass bounds on the allowed CKM4 parameter space is already significant, as shown in the results reported above. They will become more powerful as the Higgs boson searches at the Tevatron and LHC progress and when the RG analysis of the stability of the SM4 Higgs potential is generalized to account for fourth family CKM mixing. Eventually they will tighten the mixing constraints or even exclude the *perturbative* SM4 scenario. Although θ_{Cabbibo} order mixing is allowed within the 95% CL contours, the minimum χ^2 is at $\theta_{34} = 0$ and, as seen in [15], the confidence levels of the best EW fits decrease monotonically as $|s_{34}|$ increases.

Of course the underlying assumption of both the EW fits and the RG analysis of the Higgs potential is that SM4 exists as an effective field theory that can be approximately described by perturbation theory within some energy domain. This is a plausible assumption for fourth family masses below the perturbative unitarity bounds but fails for larger masses; in particular, in [15] we traced how the two loop nondecoupling corrections grow as $m_{t'}$ increases above the unitarity bound toward 1 TeV. If there is little or no hierarchy between the heavy quark threshold at $2m_{t'}$ and the scale of new strong dynamics, then the EW fits and the RG analysis both become quantitatively unreliable. In that case the LHC will encounter a new realm of strong dynamics whose exploration will make for a very rich physics program. If the fourth family quarks are very heavy, e.g., $m_Q \gtrsim 1$ TeV, and difficult or impossible to observe directly, they will give rise to a large $gg \rightarrow ZZ$ (and WW) signal in the diboson energy region $m_H^2 < s_{ZZ} < 4m_{Q_4}^2$ that could be seen at the LHC with 5σ significance over backgrounds with only $\text{O}(10) \text{ fb}^{-1}$ of integrated luminosity,[4] before direct detection would be possible.

Acknowledgements: I would like to thank Jens Erler for providing detailed information concerning the fits in [16] and Zoltan Ligeti for helpful comments.

This work was supported in part by the Director, Office of Science, Office of High Energy and Nuclear Physics, Division of High Energy Physics, of the U.S. Department of Energy under Contract DE-AC02-05CH11231

References

- [1] P. Frampton, P.Q. Hung, M. Sher, Phys.Rept.**330**:263,2000.
- [2] B. Holdom, JHEP**0708**:069,2007, arXiv:0705.1736; JHEP 0703:063,2007, hep-ph/0702037; Phys.Lett.**B686**:146-151,2010, arXiv:1001.5321; B. Holdom and Q-S Yan, arXiv:1004.3031; V.E. Ozcan, S. Sultansoy, G. Unel, ATL-PHYS-PUB-2007-018, arXiv:0802.2621; G. Burdman *et al.*, Phys.Rev.**D79**:075026,2009, arXiv:0812.0368; S. Bar-Shalom, G. Eilam, A. Soni, Phys.Lett.**B688**:195-201,2010, arXiv:1001.0569.
- [3] M.S. Chanowitz, M.A. Furman, I. Hinchliffe, Phys.Lett.**B78**:285,1978; Nucl.Phys.**B153**:402,1978.
- [4] M. Chanowitz, Phys.Lett.**B352**:376,1995.
- [5] B. Holdom, JHEP**0608**:076,2006, hep-ph/0606146; Phys.Rev.**D54**:1068,1996, hep-ph/9512298; Y. Simonov, arXiv:1004.2672.
- [6] H. Fritzsch, Phys.Lett.**B289**:92,1996; P.Q. Hung, Phys.Rev.**D77**:037302,2008; W.-S. Hou, F.-F. Lee, arXiv:1004.2359.
- [7] B. Holdom, Phys.Rev.Lett.**57**:2496,1986, E **58**:177,1987 and JHEP**0608**:076,2006; C.T. Hill, M. Luty, E. Paschos, Phys.Rev.**D43**:3011,1991; T. Elliott, S.F. King, Phys.Lett.**B283**:371-378,1992; G. Burdman, L. Da Rold, JHEP **0712**:086,2007, arXiv:0710.0623; M. Hashimoto, V. Miransky, Phys.Rev.**D80**:013004, 2009; Phys.Rev.**D81**:055014,2010; P.Q. Hung, C. Xiong, arXiv:0911.3890, arXiv:0911.3892.
- [8] W.-S. Hou, Chin.J.Phys.**47**:134,2009, arXiv:0803.1234; S.W. Ham, S.K. Oh, D. Son, Phys.Rev.**D71**:015001,2005, hep-ph/0411012; R. Fok, G.D. Kribs, Phys.Rev.**D78**:075023,2008, arXiv:0803.4207; Y. Kikukawa, M. Kohda, J. Yasuda, Prog.Theor.Phys.**122**:401-426,2009, arXiv:0901.1962.
- [9] W.-S. Hou, R. Wiley, A. Soni, Phys.Rev.Let.**58**:1608,1987; A. Arhrib, W.-S. Hou, Eur.Phys.J.**C27**:555, 2003; W.-S. Hou, M. Nagashima, A. Soddu, Phys.Rev.**D72**:115007,2007 and Phys.Rev.**D76**:016004,2007; W.-S. Hou, C.-Y. Ma, arXiv:1004.2186; S. Bar-Shalom, D. Oaknin, A. Soni, Phys.Rev.**D80**:015011,2009, arXiv:0904.1341; A. Soni *et al.*, Phys.Lett.**B683**:302,2010, arXiv:0807.1971; J.A. Herrera, R.H. Benavides, W.A. Ponce, Phys.Rev.**D78**:073008,2008. arXiv:0810.3871; M. Bobrowski *et al.*, JHEP**03**:009,2010, arXiv:0902.4883; A. Buras *et al.*, arXiv:1002.2126 and arXiv:1004.4565; O. Eberhardt, A. Lenz, J. Rohrwild, arXiv:1005.3505.
- [10] B. Holdom, JHEP**0608**:076,2006.

- [11] M. Hashimoto, Phys.Rev.**D81**:075023,2010.
- [12] H.-J. He, N. Polonsky, S-F Su, Phys.Rev.**D64**:053004,2001. e-Print: hep-ph/0102144
- [13] V.A. Novikov, L.B. Okun, A.N. Rozanov, M.I. Vysotsky, Phys.Lett.**B529**:111-116,2002, hep-ph/0111028; JETP Lett.**76**:127-130,2002, Pisma Zh.Eksp.Teor.Fiz.**76**:158-161,2002, hep-ph/0203132.
- [14] G.D. Kribs, T. Plehn, M. Spannowsky, T.M.P. Tait, Phys.Rev.**D76**:075016,2007. arXiv:0706.3718 [hep-ph]
- [15] M.S. Chanowitz, Phys.Rev.**D79**:113008,2009.
- [16] J. Erler, P. Langacker, arXiv:1003.3211.
- [17] M. Chanowitz, Phys.Rev.Lett.**87**:231802,2001, hep-ph/0104024; M. Chanowitz, Phys.Rev.**D66**:073002,2002, hep-ph/0207123. For a recent discussion see the talk posted at <http://www.ggi.fi.infn.it/talks/talk1452.pdf>, March 2010.
- [18] The ALEPH, DELPHI, L3, OPAL, SLD Collaborations, the LEP Electroweak Working Group, the SLD Electroweak and Heavy Flavour Groups, Phys.Rep.**427**:257,2006, hep-ex/0509008.
- [19] A.B. Arbuzov *et al.*, Comput.Phys.Commun.**174**:728,2006. e-Print: hep-ph/0507146.
- [20] M. Awramik, M. Czakon, A. Freitas, JHEP **0611**:048,2006, hep-ph/0608099; M. Awramik, M. Czakon, A. Freitas, G. Weiglein, Phys.Rev.**D69**:053006,2004, hep-ph/0311148.
- [21] The ALEPH, DELPHI, L3, OPAL, SLD Collaborations, the LEP Electroweak Working Group, the Tevatron Electroweak Working Group, and the SLD Electroweak and Heavy Flavour Groups, LEPEWWG/2009-01, November 2009, accessible at <http://www.cern.ch/LEPEWWG>.
- [22] W.-S. Hou, C.-Y. Ma, cited in [9].
- [23] T. Aaltonen *et al.* (The CDF and D0 Collaborations), arXiv:1005.3216, May 2010.
- [24] R. Barbieri *et al.*, Nucl.Phys.**B409**:105,1993.
- [25] C. Amsler *et al.*, Physics Letters **B667**:1,2008.
- [26] D. Abbaneo *et al.* (LEP Heavy Flavor Working Group), Eur.Phys.J.**C4**:185,1998.

- [27] H. Burkhardt, B. Pietrzyk, Phys.Rev.**D72**:057501,2005, hep-ph/0506323.
- [28] T. Teubner *et al.*, arXiv:1001.5401.
- [29] J. Erler, Phys.Rev.**D81**:051301,2010, arXiv:1002.1320
- [30] J. Erler, private communication.
- [31] P.L. Anthony *et al.* (SLAC E158 Collaboration), Phys.Rev.Lett.**95**:081601,2005.
- [32] G.P. Zeller *et al.* (NuTeV Collaboration), Phys.Rev.Lett.**88**:091802,2002;
90:239902(E),2003.
- [33] D. Mason *et al.* (NuTeV Collaboration), Phys. Rev.Lett.**99**:192001,2007.
- [34] S.G. Porsev, K. Beloy, A. Derevianko, Phys. Rev.Lett.**102**:181601,2009.
- [35] S.G. Porsev, K. Beloy, A. Derevianko, arXiv:1006.4193.
- [36] T. Aaltonen *et al.* (CDF Collaboration), Phys.Rev.Lett.**104**:091801,2010.
- [37] P.Q. Hung, M. Sher, Phys.Rev.**D77**:037302,2008; C. Flacco *et al.*, arXiv:1005.1077.
- [38] T. Yanir, JHEP**0206**:044,2002, hep-ph/0205073.
- [39] J. Alwall *et al.*, Eur.Phys.J.**C49**:791,2007, hep-ph/0607115.
- [40] M. Veltman, Nucl.Phys.**B123**:89,1977.
- [41] H. Lacker, A. Menzel, arXiv:1003.4532
- [42] See O. Eberhardt *et al.* cited in [9].